Preparation and Characterization of the Mesoporous SiO_2–TiO_2/Epoxy Resin Hybrid Materials

Shaorong Lu, Wei Chun, Jinhong Yu, Xiaowang Yang

Key Laboratory of New Processing Technology for Nonferrous Metal Materials and of Ministry of Education, Guilin 541004, People's Republic of China

Received 7 September 2006; accepted 26 November 2007
DOI 10.1002/app.27856
Published online 2 May 2008 in Wiley InterScience (www.interscience.wiley.com).

ABSTRACT: In this work, epoxy/tatania/silica ternary hybrid materials with covalent bonding interaction between polymer and inorganic phases have been prepared using titania/silica mesoporous particles, which were prepared by the sol–gel process from tetraethoxysilane (TEOS) and titanium *tetra*-butyltitanate (TBT) as precursors. The obtained hybrid particles were characterized by Nitrogen physisorption, X-ray diffraction (XRD), Fourier transform infrared spectroscopy (FTIR), etc. From the experimental results, the glass transition temperature (T_g) increases and the modulus of the modified systems decreases by adding mesoporous SiO_2–TiO_2 particles to epoxy matrix, the impact strength and tensile strength of the hybrid materials increase by 53.5% and 14% when the SiO_2–TiO_2 content is up to 3 wt %. The morphological, structure of the impact fracture surface and the surface of the hybrid were observed by scanning electron microscope (SEM) and atomic force microscopy (AFM), respectively. © 2008 Wiley Periodicals, Inc. J Appl Polym Sci 109: 2095–2102, 2008

Key words: epoxy resin; mesoporous silica–titania; sol–gel process; hybrid materials

INTRODUCTION

Organic–inorganic polymer hybrid materials have received a great deal of attention in recent years. The hybrids have organic and inorganic elements that are mixed in a molecular level, and the intimate mixing provides various properties such as hardness, abrasion resistance, adhesive strength, UV protection, etc., and could be widely used in coatings, rubbers, plastics, sealants, fibers, etc.[1–3]

Epoxy resin (EP) is one of the most important thermosetting polymer materials, which have been widely used as high performance materials, adhesives, coatings, matrices of composite materials, and electronic encapsulating materials because of their high modulus and strength, excellent chemical resistance, and simplicity in processing. However, the use of thermosetting materials is often limited by their toughness properties, which affect the durability of components and place strong constraints on design parameters. Impact resistance, fatigue behavior, and damage tolerance are some of the properties influenced. For practical applications, high strength and high toughness are required. To enhance strength and toughness, many researchers[4–11] have improved the toughness of EPs by incorporating soft particles such as rubber, thermoplastics, and hyperbranched polymer, etc., and proposed some toughening mechanisms. However, these show the lower flexural strength and Young's modulus and thermal stability over the high temperature region.

Several workers have investigated mechanical properties of particulate reinforced epoxy composites. Incorporation of rigid inorganic filler into epoxy systems is a well-known technique to improve the physical and mechanical properties.[12–16] Of paramount importance is titania–silica (Ti/Si) mixed oxides because of their properties as glasses with low thermal coefficient, catalyst supports, and catalyst.[17,18] Such Ti/Si materials would not take advantage of both TiO_2 (an n-type semiconductor and active catalyst support) and SiO_2 (high thermal stability and excellent mechanical strength), but would also extend their applications through the generation of new active sites due to the interaction of TiO_2 with SiO_2.[19] Moreover, applying of TiO_2 onto SiO_2 offers a way of obtaining a titania surface with high, thermally stable surface area, and good mechanical properties.[20]

In this study, we make an attempt to investigate the preparation of polymer hybrids containing

This article contains supplementary material available via the Internet at http://www.interscience.wiley.com/jpages/0021-8995/suppmat.

Correspondence to: S. Lu (gllushaorong@glite.edu.cn).

Contract grant sponsor: Natural Science Foundation of China; contract grant number: 50473060.
Contract grant sponsor: Natural Science Foundation of Guangxi province; contract grant number: 0447053.
Contract grant sponsor: Department of Education of Gunangxi Province; contract grant number: ([2004] 20).

mesoporous titania and silica particles, which start from hybrid xerogels containing polyethylene glycol as a pore-forming agent, then directly introduced into EP without any surface treatment. The obtained mesoporous SiO_2–TiO_2/EP hybrid materials were investigated by Fourier transform infrared spectroscopy (FTIR), dynamic mechanical analysis (DMA), differential scanning calorimetry (DSC), and atomic force microscopy (AFM), etc. The effect of the contents of mesoporous SiO_2–TiO_2 on the properties of SiO_2–TiO_2/EP hybrid materials such as the morphology, mechanical/thermal properties, and X-ray diffraction (XRD) analysis was investigated.

EXPERIMENTAL

Materials and measurement

EP (diglycidyl ether of bisphenol A, DGEBA (E-51)),Wep = 196, purchased from Yueyang Chemical Plant, China, was used without further purification. 4,4′-Diaminodiphenylsulphone (DDS, from Shanghai Chemical Reagent Company, China) had a molecular mass of 248.31 and purity >96%. Tetraethoxysilane (TEOS), 98% $Si(OC_2H_5)_4$, and titanium *tetra*-butyltitanate (TBT), $Ti(OC_4H_9)_4$ (Both chemical reagent grade) were ordered from Xilong Chemical Factory, Guangdong, China. Distilled water was used to induce the hydrolysis of the TEOS or TBT components using HCl as catalyst. Poly(ethylene glycol) (PEO) was purchased from Xilong Chemical Fractory, Guangdong, China. PEO has a quoted molecular weight of M_n = 2000, was of analytical grade and carefully got rid of water before use.

The specific surface area (S_{BET}), mean pore diameter ($\langle dp \rangle$), and specific desorption pore volumes were determined by nitrogen physisorption at 77.3 K using a NOVA 1200e Surface Area & Pore Size Analyzer (Quantachrome Instruments Corporation, USA). All calculations were performed using the associated Micromeritics software.

The Fourier transformed infrared spectroscopy (FTIR) was conducted on a Perkin–Elmer 1710 instrument at room temperature (25°C). The samples of the hybrid materials were granulated and the power was mixed with KBr pellets to press into the small flasks. The crystal behavior of the epoxy and epoxy/SiO_2–TiO_2 hybrid materials were analyzed by X-ray diffractometry (XRD: D/max-RB, Japan).

The impact strength of the cured resins was determined by a charpy impact-testing machine (XJJ-50, Chende, PRC) according to China National Standard GB1043-79. The tensile strength and tensile modulus were examined with a Shengzhen Reger RGT-5 universal testing system, at the tensile rate 2 mm/min, according to China National Standard GB1040-92. All the presented results are average of five specimens. Thermogravimetic analyses (TGA) was carried out using NETZSCH STA449 from 40 to 700°C at a heating rate of 10°C/min under nitrogen. DSC was carried out using NETZSCH DSC 204 from 50 to 270°C at a heating rate of 30 K/min under nitrogen. DMA was performed with a TA Instruments (Q800 dynamic mechanical analyzer) using 1 Hz frequency. The measurements were taken in the interval −70 to 250°C at a heating rate of 5°C/min. The three point bending mode was chosen and the dimensions of the specimen were 48 mm × 5 mm × 2.5 mm. Transmission electron micrograph was observed with a JEOL-2010 instrument at a high voltage of 120 kV. SEM studies of the fracture surface of the impact specimens were carried out with a JEOL JSM-6380 LV instrument. The surfaces were gold-coated prior to the measurements. AFM was carried out using AJ-IIIa analyzer (Shanghai AJ Nano-Science Development Co.) and the tapping mode was utilized. The scan size was about 7.2 μm × 7.2 μm.

Preparation of mesoporous SiO_2–TiO_2[21]

The mesoporous SiO_2–TiO_2 materials were prepared through a sol–gel process by using Polyethylene glycol as a pore-forming agent. The inorganic sol–gel was prepared by stirring the mixture of a calculated amount of TEOS, TBT, ethanol, water, and HCl at room temperature for 3 h. In a typical synthesis, 10 g polyethylene glycol and 0.1 mol TEOS were partially hydrolyzed in ethanol (ethanol: TEOS molar ratio = 0.5) with magnetic stirring in the presence of aqueous HCl as catalyst. The amount of water used was that calculated in order to have a H_2O: ($MSiO_2$+$MTiO_2$): HCl molar ratio = 0.5 : 1 : 0.01. The solution was stirred for about 20 min at room temperature. Once the solution turned clear, a previously calculated amount of TBT was added dropwise, and the solution was stirred for 2 h at room temperature. The mixture was transferred into a 200-mL beaker and covered with parafilm for a few days to allow the evaporation of small molecules. The resulting xerogels were then dried at 60°C for 24 h. Finally, the organic material was removed by calcinations at 600°C for 4 h (heating rate 10°C/min).

Curing procedure

SiO_2–TiO_2 particles were dispersed into epoxy in given weight percent by using ultrasonic cleaner. Three part of curing agent DDS per 10 parts of epoxy by weight were then gently mixed into the systems. The obtained mixtures were degassed in vacuum at 130°C for about 20 min. The resulting mixture was then cast into a preheat mold coated with silicone resin. All samples were cured at 130°C for 2 h, 170°C for 2 h, and 190°C for 2 h.

TABLE I
Structure Properties of Mixed Oxides for Different SiO_2–TiO_2 Contents

Sample	Composition SiO_2/TiO_2 (w/w)	A_{BET} (m^2/g)	V (cm^3/g)	D (Å)
1	100/0	441.8	0.22	16.9
2	75/25	406.7	0.12	16.8
3	50/50	297.4	0.15	15.3
4	25/75	208.8	0.06	15.3
5	0/100	183.4	0.10	13.0

A_{BET}, surface area; V, pore volume; D, pore diameter.
PEO/(SiO_2–TiO_2) = 0.5M in precursor sol.

RESULTS AND DISCUSSION

Textural properties of mixed oxides SiO_2–TiO_2

The texture and porosity of the materials determined from the adsorption and desorption isotherms is shown in Table I. The results show that all samples with different SiO_2–TiO_2 weight ratio, but maintained a constant PEO/(SiO_2–TiO_2) molar ratio (0.5 : 1) in the mixed sol. The results of Table I show that mesoporous SiO_2/TiO_2 materials with surface areas between 183 and 441 m^2/g. The surface area increase with decreasing titanium content, pore volume, ~ 0.22 cm^3/g, as well as pore diameter, 15–16 Å, remain relatively constant. The surface area decrease is probably due to an accelerated condensation between the inorganic particles in the sol, decreasing the total PEO incorporated in the resulting network with TBT contents increasing.[22]

FTIR spectra

The simplest way to determine the formation of Ti—O—Si bonds is by using FTIR spectroscopy. The FTIR spectra of pure EP, SiO_2–TiO_2 and EP/SiO_2–TiO_2 hybrid material are showed in Figure 1. Figure 1(a) shows that the characteristic peaks of the symmetric the hydroxyl-stretching band of EP appears at 3507 cm^{-1} and oxirane absorption at 915 cm^{-1}. After the introduction SiO_2–TiO_2 inorganic component, the low wavenumber region of the IR absorption spectrum has been used extensively to characterize SiO_2–TiO_2 mixed oxides. According to the data [Fig. 1(b,c)], vibration bands are observed that the broad and strong absorption bands in the range of 400–850 cm^{-1} corresponding to Ti—O—Ti network, and 920–1100 cm^{-1} corresponding to the characteristic of Si—O—Si and Si—O—Ti networks, and the bond at around 952 cm^{-1} is due to vibrations of silica perturbed by the presence of titania, and is an indication of the formation of these bonds, which has been discussed in detail in the literature.[23] The band near 3400 cm^{-1} is the characteristic band of the residual Ti—OH and Si—OH groups in the hybrid materials.

Mechanical properties

Mechanical properties of the hybrid materials are shown in Table II. As the loading of mesoporous SiO_2–TiO_2 particles increases to 3 wt %, impact strength and tensile strength of the hybrid materials increase by 53.5% and 14% as compared to the pure EP. But when the loading of mesoporous SiO_2–TiO_2 was further increased, the impact strength and tensile strength both decrease. The strength and the

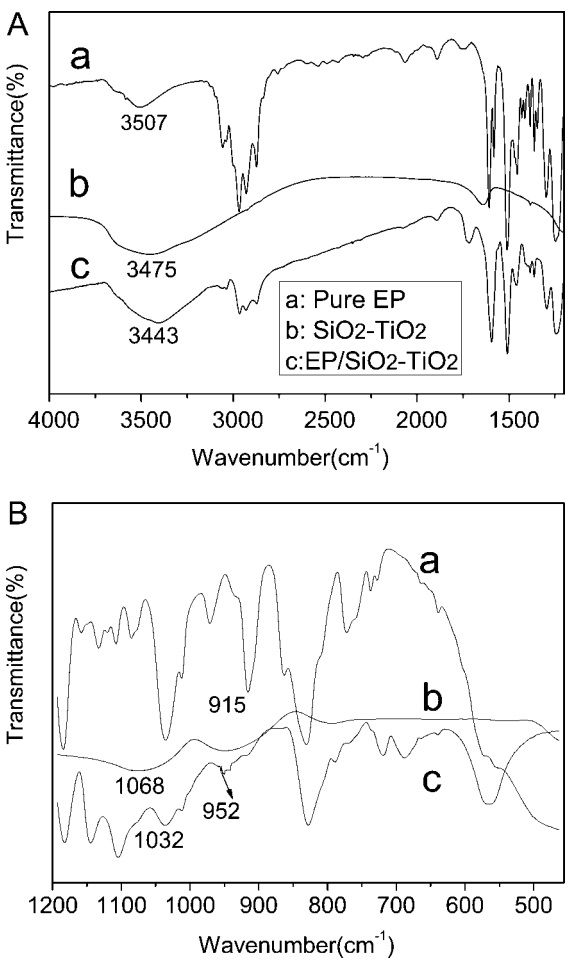

Figure 1 FTIR spectra of (a) Pure EP; (b) SiO_2–TiO_2; (c) EP/SiO_2–TiO_2.

TABLE II
Mechanical Properties of EP/SiO_2–TiO_2 Hybrid Materials

SiO_2–TiO_2 content (wt %)	Impact strength (kJ/m^2)	Tensile strength (MPa)	Tensile modulus (MPa)
0	11.6	55.9	433.8
1	14.9	58.1	509.6
2	16.8	61.2	609.4
3	17.8	63.7	545.4
4	16.3	58.2	595.7
5	14.9	56.3	455.7
3[a]	15.6	57.4	589.8
3[b]	12.8	53.7	567.4

All mesoporous SiO_2–TiO_2 mixed oxides samples are heated at 600°C and sample of SiO_2/TiO_2 (75/25 w/w).
[a] Mesoporous SiO_2, A_{BET} (m^2/g): 441.8.
[b] Mesoporous TiO_2, A_{BET} (m^2/g): 183.4.

toughness of the hybrid materials are dependent on the crosslinking density in an appropriate range of the crosslinking density, the crosslinks display the strengthening and toughening effects. A possible explanation of these results may be due to some special interactions (most likely the reaction between hydroxyl or oxirane groups of terminated EP and the surface hydroxyl groups of the mesoporous SiO_2–TiO_2 particles) between the EP and the mesoporous SiO_2–TiO_2 particles. When the material is subjected to an impact test, the epoxy/SiO_2–TiO_2 hybrid materials have generated microphase separated for introducing of the mesoporous SiO_2–TiO_2 particles, which may induce epoxy matrix yielding deformation and resistance to crack propagation. For this reason, the impact energy of the epoxy matrix is expected to increase significantly as the mesoporous SiO_2–TiO_2 particles are introduced, and resulted in toughening of the mesoporous SiO_2–TiO_2/epoxy hybrid materials enhancing. Above 3 wt % of SiO_2–TiO_2 content, however, the impact strength decreased due to the aggregation of mesoporous SiO_2–TiO_2 particles in epoxy matrix. Some supporting methods for this explanation are given in AFM and SEM.

XRD analysis

XRD patterns for mesoporous SiO_2–TiO_2 and epoxy/SiO_2–TiO_2 hybrid material are given in Figure 2. XRD analysis was carried out on mesoporous SiO_2–TiO_2 mixed oxides heated at 600°C and sample of SiO_2/TiO_2 (75/25 w/w).The XRD pattern of Figure 2(a) displays a very broad hump peak, the contact angle was around 2θ ranging between 15° and 35°, originating from amorphous phase of SiO_2–TiO_2, and do not show crystallization may be explained on the basis of an extensive Si—O—Ti connectivity,

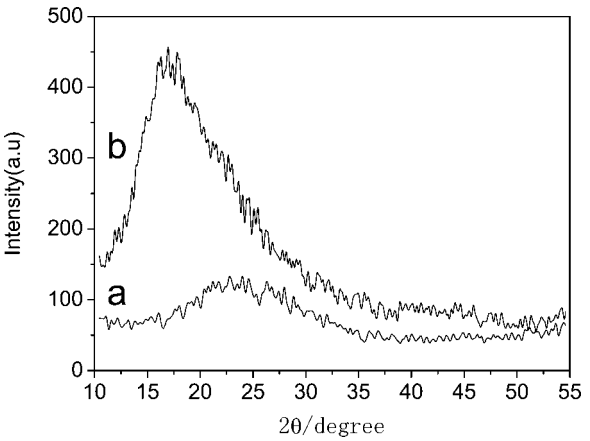

Figure 2 X-ray diffraction patterns of (a) SiO_2–TiO_2 and (b) EP/SiO_2–TiO_2 hybrid material.

i.e., titania domains is too small to crystallize. For the epoxy/SiO_2–TiO_2 hybrid material [Fig. 2(b)], the diffraction patterns shows only a broadly amorphous peak (2θ = 10–30°) derived from homogeneously amorphous SiO_2–TiO_2 matrix. This result indicates that the complete and homogeneous mixing of SiO_2–TiO_2 and matrix, and inorganic phase caused by balanced hydrogen bonding interaction in hybrid systems result in the disappearance of the crystallinity of epoxy/SiO_2–TiO_2 hybrid material. This also indicates that SiO_2 and TiO_2 do not form sufficiently large clusters for XRD during epoxy curing process. Thus, the introduction of SiO_2 and TiO_2 disrupt the epoxy intermolecular regularity.

Thermal behavior

Figure 3 shows the DSC thermograms of EP and its different SiO_2–TiO_2 contents hybrid materials. All

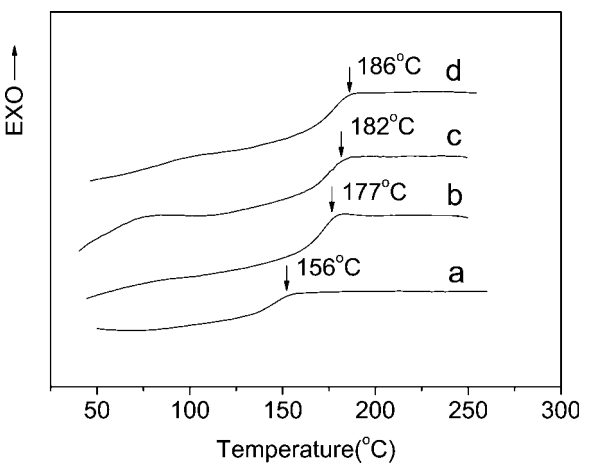

Figure 3 DSC curves of the pure epoxy and mesoporous EP/SiO_2–TiO_2 hybrid materials. (a) Pure EP;(b) 1 wt % EP/SiO_2–TiO_2; (c) 3 wt % EP/SiO_2–TiO_2; (d) 5 wt % EP/SiO_2–TiO_2.

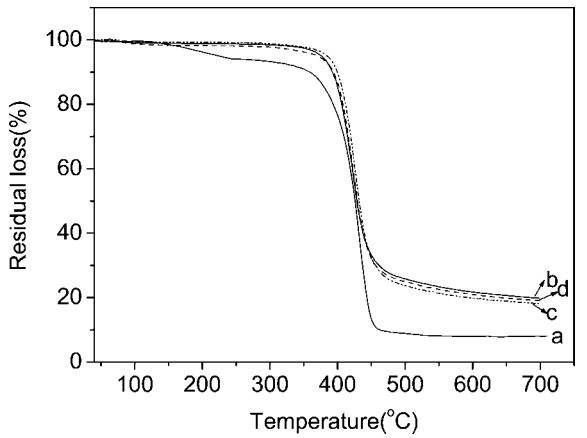

Figure 4 TGA curves of the pure epoxy and mesoporous EP/SiO_2–TiO_2 hybrid materials. (a) Pure EP; (b) 1 wt % EP/SiO_2–TiO_2; (c) 3 wt % EP/SiO_2–TiO_2; (d) 5 wt % EP/SiO_2–TiO_2.

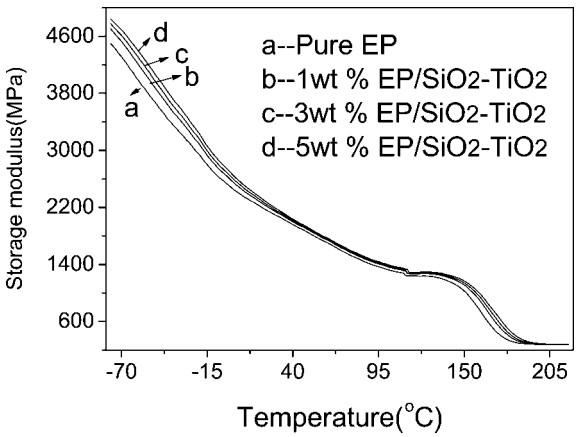

Figure 5 The plots of DMA dynamic storage modulus as functions of temperature for the pure epoxy and EP/SiO_2–TiO_2 hybrid materials.

three samples present higher glass transition temperatures (T_g) than 156°C of the pure epoxy. Moreover, the T_g increases with the increasing SiO_2–TiO_2 contents. This was due to the fact that epoxy matrix could penetrate through mesoporous SiO_2–TiO_2 particles and transform to SiO_2–TiO_2 network, with higher the mesoporous SiO_2–TiO_2 contents in the matrix, stronger SiO_2–TiO_2 network should be obtained, and the immobilized chains of epoxy bonding with the rigid SiO_2–TiO_2 domains. The glass transition behavior was further confirmed by DMA.

Figure 4 shows the TGA thermograms of results of the thermal decomposition of the pure EP and epoxy/SiO_2–TiO_2 hybrid materials. It is obvious that the initial thermal decomposition temperature of the epoxy/SiO_2–TiO_2 is higher than that of the pure EP, which is 379°C while the epoxy/SiO_2–TiO_2 is 394°C when SiO_2–TiO_2 content is 5 wt %. The results may attribute to the strong interaction between the polymer chains and inorganic particles and consequently preventing epoxy from thermal decomposition. At the temperature of 700°C, the char yield of pure epoxy is 7.81 wt % and that of the epoxy/SiO_2–TiO_2 5 wt % is 19.8 wt %. The experimental residues are much higher than the theories values because some of the epoxy chains are trapped in the mesoporous SiO_2–TiO_2 particles, which confirm the existence of strong interaction between the two phases.

Dynamic mechanical properties

The temperature dependence of dynamic mechanical properties of the epoxy/SiO_2–TiO_2 hybrid materials containing different amount of silica and titania network are shown in Figure 5. In the glassy region and in the rubbery region, the storage modulus of hybrid materials showed little increased by addition of the mesoporous SiO_2–TiO_2 to EP. This behavior is probable that some special interaction (most likely the reaction between the hydroxyl groups of epoxy and the surface hydroxyl groups of the mesoporous SiO_2–TiO_2 particles) between the polymer and the mesoporous SiO_2–TiO_2 are formed, and increased the crosslinked density of the composites (compared to pure epoxy) by adding mesoporous SiO_2–TiO_2 particles. The results suggest that the mobility of the epoxy chains was restricted by the interaction of the fairly dispersed SiO_2–TiO_2 domains with the matrix epoxy, as well as the degree of crosslinking increased with increasing the amount of the mesoporous SiO_2–TiO_2 particles.

Figure 6 shows the dynamic mechanical spectra for tan δ of the epoxy and mesoporous epoxy/SiO_2–TiO_2 hybrid materials. When compared with the pure epoxy, the peak tan δ values for modified system appears to be slightly decreased with mesoporous SiO_2–TiO_2 content increasing. The tan δ peak

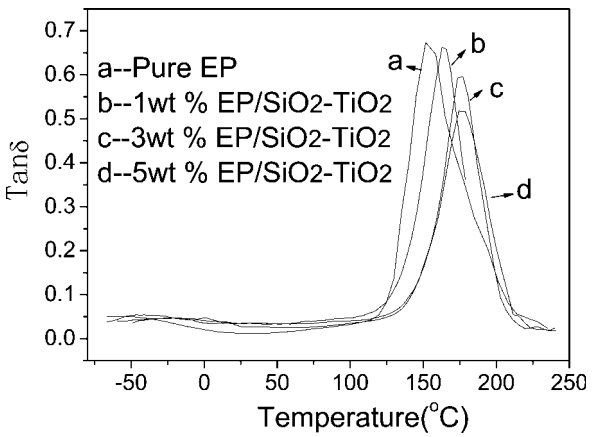

Figure 6 The plots of DMA tan δ as functions of temperature for the epoxy and EP/SiO_2–TiO_2 hybrid materials in the temperature range of −70 to 250°C.

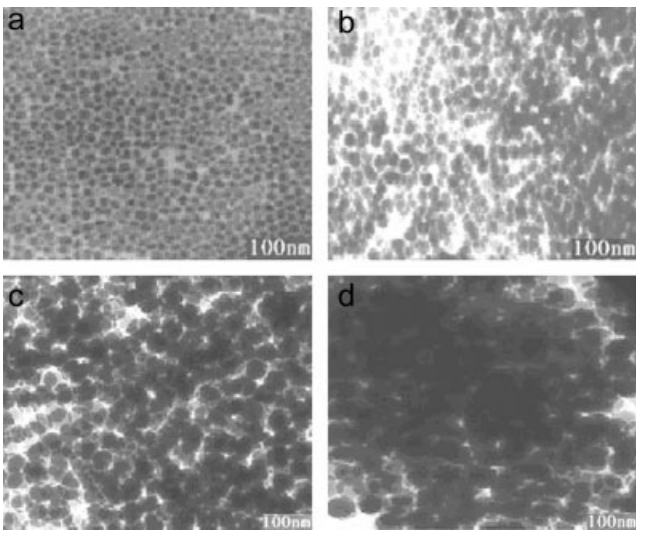

Figure 7 TEM photograph of (a) porous SiO_2–TiO_2; (b) 1 wt % SiO_2–TiO_2/epoxy hybrid material; (c) 3 wt % SiO_2–TiO_2/epoxy hybrid material; (d) 5 wt % SiO_2–TiO_2/epoxy hybrid material.

temperature for the hybrid materials is considerably higher than that of the pure system. The addition of SiO_2–TiO_2 in matrix made it difficult to move the polymer chain. Therefore, the peak tan δ values decreased and glass transition temperatures (T_g) were shifted to higher temperature. The reason for this may be attributed to a loss in the mobility of the chain segments of EP, resulting from some special interaction (mesoporous SiO_2–TiO_2 particles/matrix interaction). The particles surface-to-surface distance should be relatively small and chain segments movement may be restricted.

Morphology

TEM analysis

Since the mechanical properties of composites depend strongly on the dispersion degree of the porous SiO_2–TiO_2 powder in the polymer matrix, TEM techniques were employed to investigate the dispersion of SiO_2–TiO_2 powder in EP matrix. Figure 7 shows the TEM micrographs of porous SiO_2–TiO_2 powder and its hybrid material. For porous SiO_2–TiO_2 powder [Fig. 7(a)], the micrograph shows irregularly shaped spherical particles with loose and discrete structure. Distribution of particle size of porous SiO_2–TiO_2 over a broad range was observed with the average size of 42 nm. As for the hybrid material [Fig. 7(b)], it can be found that the porous SiO_2–TiO_2 preserves the original spherical morphology, and it was clearly observed homogeneously dispersing in the EP matrix. The results obtained from the TEM micrographs showed that the average particle size was about 80 nm for the case of 1 wt % SiO_2–TiO_2 particles, while mono-disperse and nonagglomeration of the SiO_2–TiO_2 particles being observed from the TEM micrographs. However, increase in SiO_2–TiO_2 particles contents reached up to 3 wt % and 5 wt %, respectively. There is only a low degree of agglomeration, large single, as well as small agglomerated nanoparticles are observed in polymer matrix, shown in Figure 7(c,d). The particle size calculations were made from the TEM micrographs and were found to be about 100–200 nm. Since SiO_2–TiO_2 particles and epoxy are blend in the macroscopic level, the mechanical testing results demonstrate the properties of the hybrid material with a uniform distribution of nanoparticles are greatly improved,[24] the experimental results can be also seen in Table II.

Atomic force microscopy

AFM was utilized to study the surface morphology of the representative hybrid films. Figure 8 shows the representative images of different porous SiO_2–TiO_2 particles contents. The bright domains are attributed to the silica phase, while the dark domains are assigned to the epoxy network. In the

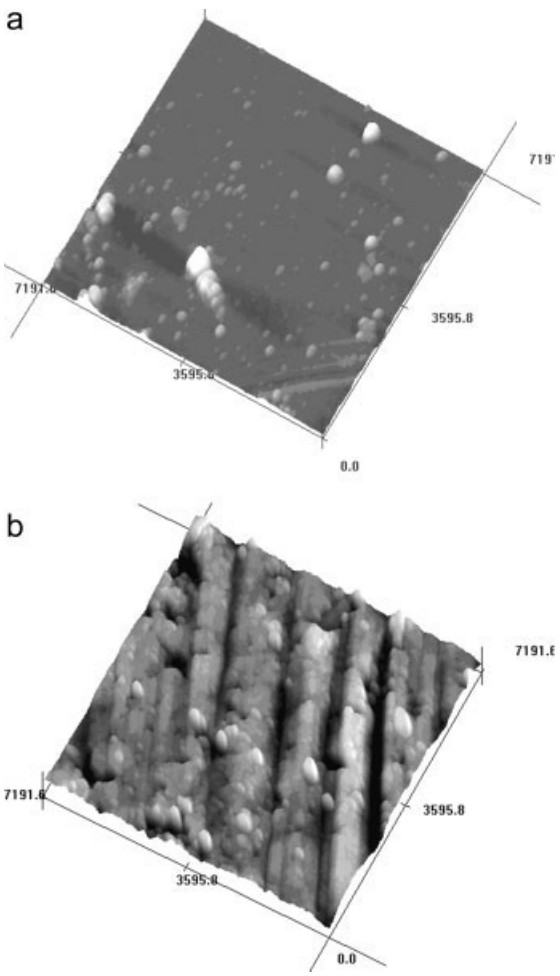

Figure 8 Typical AFM topographic images of composite with (a) 1 wt % SiO_2–TiO_2 and (b) 3 wt % SiO_2–TiO_2.

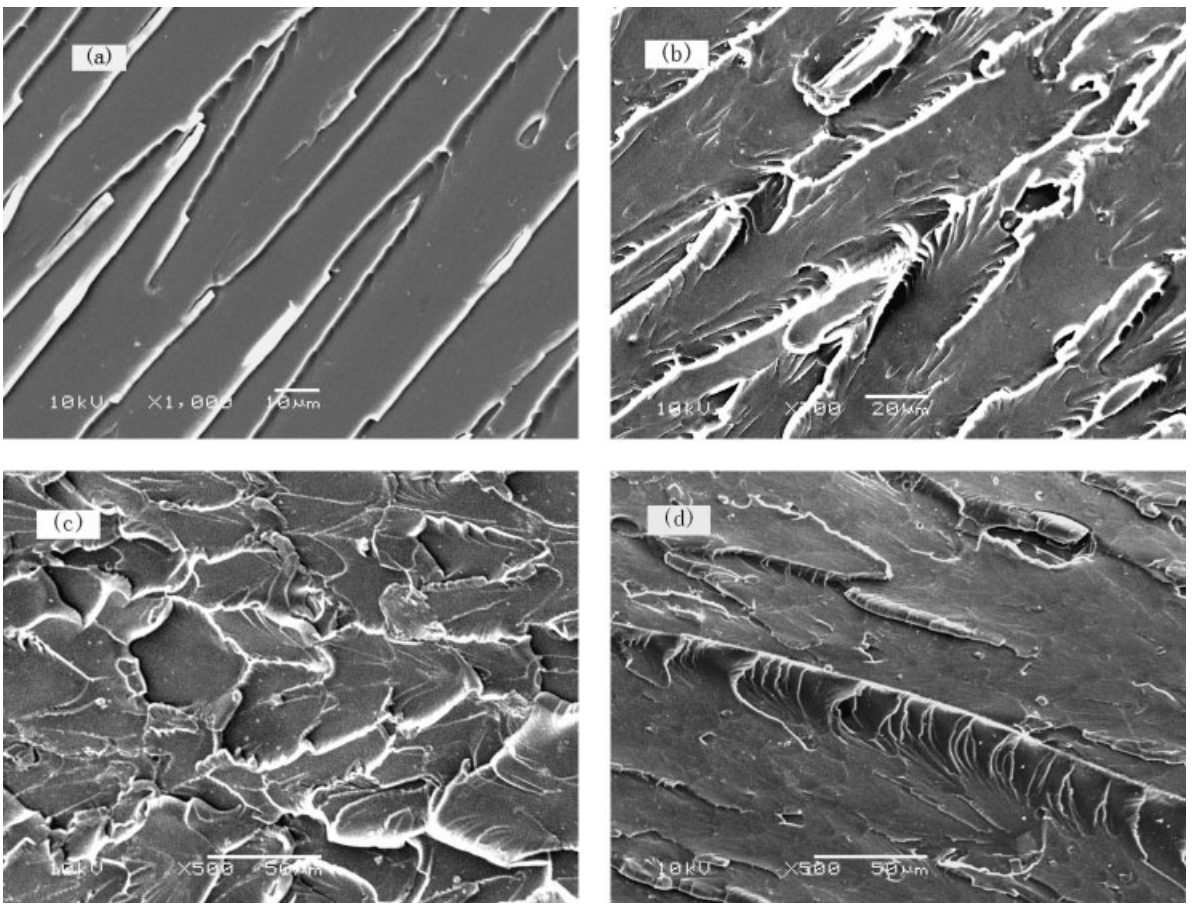

Figure 9 SEM photography of the fracture surface of hybrid materials (a) pure EP; (b) 1 wt % SiO_2–TiO_2; (c) 3 wt % SiO_2–TiO_2; (d) 5 wt % SiO_2–TiO_2.

3D images, Figure 8(a) shows that the organic and inorganic phase are strictly interconnected with no major macroscopic phase separation that might have occurred during the curing process. But the AFM topographic of Figure 8(b) reveals a typical phase-segregated morphology. With increasing the porous SiO_2–TiO_2 particles content, significant changes were observed in the surface morphology. The porous SiO_2–TiO_2 particles are segregated from the epoxy phase to form larger domains called ''island" in the ''sea-island" structure, which may be formed by the microphase separation. The 3D images also indicate that the surface roughness (RMS) of the Figure 8(a) is 21.6 nm, while Figure 8(b) is 52.3 nm, the RMS values of the composites obviously increase with increasing contents of SiO_2–TiO_2 particles. These images may demonstrate that a strong bond has been formed between the porous SiO_2–TiO_2 particles and the epoxy matrix in the composites.

Scanning electron microscopy

SEM was used to characterize the particle dispersion and fracture surfaces of pure EP and the hybrid materials with containing difference porous SiO_2–TiO_2 contents. The crack growth regions are shown in Figure 9. From the photograph [Fig. 9(a)], one can see that the fracture surface for control system is quite different from that of the modified systems, it was very smooth and with uniform crack direction, and reveals the characteristic of brittle fracture and accounts for its poor impact strength. As for the modified systems Figure 9(b–d), which indicate tough fracture, and the fracture cross section of every hybrid material exhibits a good dispersion state of mesoporous SiO_2–TiO_2 particles. The fracture surface of Figure 9(b) shows branches and appears rougher than that of the pure epoxy system. Its impact strength gets considerable improvement correspondingly. Fracture surfaces of Figure 9(c,d) present large and deep cavities, which are generally characteristic of rubber-modified EPs. These cavities represent the initial position of the rubber particles, which were pulled out or broken during the fracture process. These cavities are firmly attached to the epoxy matrix, resulting in a good adhesion and a strong interface between the mesoporous SiO_2–TiO_2 particles and epoxy matrix phase. A mechanism, proposed by Pearson et al.,[25] and reported by Pearson and Yee[26] and which seems to fit relatively well

with the results of the present study suggests that the fracture resistance increases, arising from a great extent of energy-dissipating deformation occurring in the material in the vicinity of the crack tip. Such results explain the increase in the epoxy roughness, and the most probable mechanism is based on internal cavitation of the SiO_2–TiO_2 particles, which like the rubber particles, followed by localized plastic deformation. The result shows that branches and cavities appearance on the fracture surface played an important role in improving impact strength. The rough fracture surface of the hybrid materials result from smaller phase separation and the special interaction between the SiO_2–TiO_2 particles and the polymer that constrains the polymer chains' mobility and the efficiency of the rearrangement.

CONCLUSIONS

From the results and the discussion in the preceding sections, it is possible to draw the following main conclusions:

1. DSC and TGA curves revealed a higher thermal stability of the hybrid materials, and the fracture surfaces of all hybrid materials exhibit the character of tough fracture feature.
2. Adding mesoporous SiO_2–TiO_2 particles decreases the modulus and increases the glass transition temperature of the EP.
3. The incorporation of mesoporous SiO_2–TiO_2 particles in the epoxy matrix brings about the impact strength and tensile strength of the hybrid materials increases by 53.5% and 14% when the SiO_2–TiO_2 content is up to 3 wt % due to formation of a strong interface between the filler and matrix.

References

1. Zhang, M. Q.; Rong, M. Z.; Zheng, Y. X.; Zeng, H. M.; Friedrich, K. Polymer 2001, 42, 3301.
2. Singh, R. P.; Zhang, M.; Chan, D. J Mater Sci 2002, 37, 781.
3. Xie, X.-L.; Liu, Q.-X.; Li, R. K.-Y.; Zhang, Q.-X.; Yu, Z.-Z.; Mai, Y.-W. Polymer 2004, 45, 6665.
4. Hemi, N. J Appl Polym Sci 1986, 31, 15.
5. Kinlosh, A. J.; Shaw, H. Polymer 1983, 24, 1341.
6. Manzione, L. M.; Gillham, J. K. J Appl Polym Sci 1981, 26, 889.
7. He, S.; Shi, K.; Bai, J.; Zhang, Z.; Liang, L.; Du, Z.; Zhang, B. Polymer 2001, 42, 9641.
8. Zhang, B.-L.; Tang, G.-L.; You, Y.-C.; Du, Z.-J.; Yang, J.-F.; Huang, J.-F. Eur Polym J 2000, 36, 205.
9. Zhang, B.-L.; Tang, G.-L.; Shi, K.-Y.; Du, Z.-J.; Huang, J.-F. J Appl Polym Sci 1999, 71, 177.
10. Ratna, D.; Simon, G. P. Polymer 2001, 42, 8833.
11. Boogh, L.; Pettersson, B.; Manson, J.-A. E. Polymer 1999, 40, 2249.
12. Lu, S.; Zhang, H.; Zhao, C. J Appl Polym Sci 2006, 101, 1075.
13. Lu, S.-R.; Zhang, H.-L.; Zhao, C.-X.; Wang, X.-Y. Polymer 2005, 46, 10484.
14. Lu, S.-R.; Zhang, H.-L.; Zhao, C.-X.; Wang, X.-Y. J Mater Sci 2005, 40, 2815.
15. Lu, S.-R.; Zhang, H.-L.; Zhao, C.-X.; Wang, X.-Y. J Macromol Sci Part A: Pure Appl Chem 2005, 42, 1691.
16. Kang, S.; Hong, S., II.; Choe, C. R.; Park, M.; Rim, S.; Kim, J. Polymer 2001, 42, 879.
17. Retuert, J.; Quijada, R.; Arias, V.; Yazani-Pedram, M. J Mater Res 2003, 18, 487.
18. Pabón, E.; Retuert, J.; Quijada, R. Microporous Mater 2004, 67, 195.
19. Gao, X.; Wachs, I. Catal Today 1999, 51, 233.
20. Quaranta, N. E.; Sorial, J.; Corberán, V. C.; Fierro, J. L. G. J Catal 1997, 171, 1.
21. Pabón, E.; Retuert, J.; Quijada, R, Zarate, A. Microporous Mater 2004, 67, 195.
22. Pabón, E.; Retuert, J.; Quijada, R. Microporous Mesoporous Mater 2004, 67, 195.
23. Sadlter Research Laboratories. Inorganics IR Grating Spectra, Vols. 1–2; Philadaphia: Sadlter, 1965; Y249k.
24. Kansy, J.; Consolati, G.; Dauwc, C. Radiat Phys Chem 2000, 58, 427.
25. Pearson, R. A.; Albent, F. Polymer 1993, 34, 36589.
26. Pearson, R.A.; Yee, A. F. J Mater Sci 1986, 21, 2475.